2.3 Monitoring of Antigen-Specific Humoral Immune Responses by Enzyme-Linked Immunosorbent Assay (ELISA) Using NY-ESO-1 Antigen as an Example

1. Full-length NY-ESO-1 protein and control proteins including dihydrofolate reductase (DHFR) are supplied in 8 M urea or PBS and diluted to a final concentration of 1 μg/mL (Ludwig Institute for Cancer Research, New York branch). Protein dilutions are prepared in PBS.
2. The second antibody: goat anti-human IgG-AP (Alkaline Phosphatase)-conjugate (Southern Biotech, Inc. Birmingham).
3. AttoPhos AP Fluorescent Substrate (Promega).
4. AttoPhos buffer to reconstitute the AttoPhos Substrate (Promega).
5. Ready to use AttoPhos working solution: weigh 36 mg Attophos substrate, add to 60 mL Attophos buffer, store at 4 °C up to 1 month.
6. Blocking buffer (5 % nonfat dry (NF) milk in PBS): 500 mL PBS, 150 μg sodium azide and 25 g NF-milk fortified with Vitamins A&D.
7. Wash-buffers: 1× PBS; 1× PBS and 0.1 % Tween-20 (Tw20).
8. Stop solution: 2 N NaOH (in distilled water).
9. A pool of healthy donor sera.
10. ELISA plates (FluoroNunc Maxisorp ELISA plates, Thermo Scientific, Rochester, NY).
11. Microplate Washer ELx405 series (Biotek).
12. Biostack, automated microplate stacking device (Biotek).
13. Microplate ELISA reader (Synergy L, Biotek).

2.4 Monitoring of Antigen-Specific Cellular Responses by Tetramer and Intracellular Cytokine Staining

1. Fluorochrome-labeled antibodies: CD3 PE-Cy7, CD45RA ECD, CD4 ECD (Beckman Coulter); CCR7 FITC (R&D system); CD28 PerCPCy5.5 and CD3 Pacific Blue (BD Biosciences); and CD8 APC-AF750, CD27 APC, IL-2 APC, MIP1-beta PE, TNF-alpha PE-Cy7, and IFN-gamma FITC (BD Pharmingen).
2. Fluorochrome labeled tetramers: PE-NY-ESO-$1_{94\text{-}102}$ (MPFATPMEA) loaded HLA/B*3501, and PE-NY-ESO-$1_{157\text{-}165}$ (SLLMWITQC) loaded HLA/A0201 tetramer (Tetramer Core, Ludwig Institute of Cancer Research, Lausanne Branch, Switzerland). MHC class I negative tetramer control (Beckman Coulter). Concentration of each tetramer was determined by the staining on thawed frozen tetramer positive T cells.
3. NY-ESO-1 overlapping peptides (20-mer overlapped by ten amino acids) (JPT Peptide Technologies GmbH, Berlin, Germany). Peptides were resuspended in DMSO/PBS at the final concentration of 10 % (vol/vol) and stored at −20 °C. Peptides were thawed the day of the assay and diluted to the required concentration. They were never frozen nor thawed more than once.

4. DAPI (4′ 6-diamino-2-phenylindole, Dihydrochloride) nucleic acid stain (Invitrogen).
5. Interleukin (IL)-2 (10 IU/mL, Chiron, Emeryville).
6. IL-15 (10 ng/mL, R&D Systems).
7. Brefeldin A and monensin to block cytokine secretion (BD Bioscience).
8. PE-Cy5-CD107a antibody for detection of degranulating lymphocytes (5 μL/mL BD Pharmingen).
9. Mark I Irradiator (JL Shepard and Associated, San Fernando CA).

2.5 Myeloid-Derived Suppressor Cell Flow Phenotype Staining

1. Lineage-specific antibody (CD3/CD16/CD19/CD20/CD56) cocktail-FITC conjugate (special-ordered BD Pharmingen).
2. The following fluorochrome labeled other antibodies: CD14-PerCP Cy5.5, CD11b-APC Cy7, and CD33-PE-Cy7 (BD Pharmingen); and HLA-DR-ECD (Beckman Coulter).
3. Isotype controls: the appropriate fluorochrome-conjugated mouse IgG_1, IgG_k, IgG_{2a}, or IgG_{2bk} from same companies (BD Pharmingen and Beckman Coulter).

3 Methods

3.1 Blood Collection, Cell Separation, and Cryopreservation

1. Collect whole blood from healthy donors or patients in Vacutainer® Cell Preparation Tubes (CPT™).
2. Spin CPT tubes at 1,000 × *g* average (~2,500 rpm Beckman GH-3.8 rotor), slow acceleration, no brake, at room temperature for 25 min.
3. Collect the plasma to be used in other experiments. Harvest the interface and pool cells from interfaces in several 15 mL centrifuge tubes. Top off with RPMI media.
4. Spin at 600–650 × *g* (1,500 rpm Beckman GH-3.8 rotor) in cold centrifuge (4 °C) for 10 min.
5. Aspirate supernatant and resuspend pellet in RPMI media before each wash (approximately 45 mL).
6. Spin at 200–235 × *g* (1,100 rpm Beckman GH-3.8 rotor) in cold centrifuge (4 °C) for 10 min.
7. Aspirate supernatant and resuspend pellet in RPMI media before each wash (approximately 45 mL).
8. Repeat **steps 6** and 7 twice.
9. Count cells either using Trypan Blue at appropriate dilution to count ~100 cells or Guava cell analyzer.
10. For cryopreservation resuspend peripheral blood mononuclear cells (PBMC) in autologous plasma or human serum albumin with 10 % DMSO, keep frozen at −80 °C for 2–3 days and then store in liquid nitrogen.

3.2 Monitoring of Activated T Cell Subpopulations by Flow Phenotype Staining

1. Wash 0.5 million PBMCs with 2 mL FACS buffer.
2. Resuspend the cells in 50 μL FACS buffer and stain with 1 μL ICOS-PE-Cy7 antibody and the following antibodies: 3 μL CD3-Pacific Blue, 1 μL CD4-ECD, 1 μL CD8-PE-Cy5 and 2 μL CD25-PE. Incubate at 4 °C for 30 min.
3. Rewash the cells with FACS buffer, fix and permeabilize the cells with 250 μL 1× fixation/permeabilization solution at 4 °C for 30 min before washing with 2 mL 1× permeabilization buffer.
4. Add 5 μL FOXP3-APC antibody at 4 °C for 60 min before a final washing with 1× permeabilization buffer.
5. Resuspend the cells in 400 μL FACS buffer and perform flow cytometry analysis and acquire data on a CYAN flow cytometer with Summit software.
6. Perform data analysis by using FlowJo software.
7. Use isotype controls for the appropriate fluorochrome-conjugated mouse IgG_{1a} or IgG_{2a} for setting up the gate (*see* **Note 1**).

3.3 Monitoring of Antigen-Specific Humoral Immune Responses by ELISA

1. Prepping of ELISA plates: Add 1 μg/mL of desired antigen (e.g., NY-ESO-1) in PBS (30 μL/well). Incubate overnight at 4 °C or at room temperature for 2 h.
2. Shake off contents of plates, wash three times with 1× PBS and blot dry with paper towels.
3. Block with 5 % NF milk in PBS (30 μL/well) and incubate at 4 °C overnight or at room temperature for 2 h.
4. Shake off contents and wash as in **step 2**.
5. Prepare human serum dilution in blocking buffer in 96-well dilution trays. Usual serum dilutions are fourfold: 1:100, 1:400, 1:1,600, etc.
6. Shake off last wash, blot dry with paper towel and add serum dilutions (30 μL/well) incubate at 4 °C overnight.
7. Shake off contents and wash 3× with 1× PBS and 0.1 % Tw20, and 3× with 1× PBS using Microplate Washer and Biostack.
8. Shake off last wash, blot dry with paper towel and add second antibody (goat anti-human IgG-AP) at appropriate dilution 1:4,000 in blocking buffer (30 μL/well) and incubate at room temperature for 1 h.
9. Shake off contents and wash as in **step 7**.
10. Shake off last wash, blot dry, and add 30 μL AttoPhos working solution containing AP substrate and incubate in dark for 30 min.
11. Stop color development by adding 15 μL stop solution (2 N NaOH).

12. Fluorescence signal (Excitation at 450/50 nm and Emission at 580/50 nm with gain of 25) is measured using ELISA plate reader with Biostack (Optics position top 510 nm, lightsource Tungsten, detection method fluorescence, read type endpoint) (*see* **Note 2**).

3.4 Monitoring of Tumor Antigen-Specific Cellular Responses by Tetramer and Intracellular Cytokine Staining

3.4.1 In Vitro Stimulation with T Cell-Specific Peptides

1. Resuspended thawed PBMCs in 10 % pooled human serum (PHS) in RPMI 1640 medium and plate at 2.5×10^6 cells per well.
2. Pulse $2.5 \times 10e^6$ autologous PBMCs with 20-mer NY-ESO-1 overlapping peptides (10 μg/mL) at room temperature for 1 h, then irradiate with 30 Gy and culture with the responder cells at 1:1 ratio.
3. The culture medium contains IL-2 (10 IU/mL) and IL-15 (10 ng/mL). Change media every 2–3 days during the in vitro stimulation.
4. After 10 days of in vitro culture, harvest the cells and analyze by flow cytometry for tetramer staining and intracellular cytokine staining.

3.4.2 Tetramer Staining

1. Incubate $5 \times 10e^5$ cells with 0.5 μL of corresponding tetramer in 50 μL FACS buffer, 0.05 mM EDTA, 0.01 % sodium azide at 37 °C for 15 min, followed by the surface antigen-specific antibodies at room temperature for another 15 min.
2. Wash the cells with FACS buffer once and resuspend in 300 μL FACS buffer for flow cytometric acquisition.
3. Cells are considered positive for tetramer staining when they form a clear population with mean fluorescence intensity that is ≥1 log above the MHC Class I negative tetramer control (*see* **Note 3**).
4. Collect events ($\geq 10^5$) after live gating on lymphocytes by forward and side scatter. Use DAPI stain to gate out dead cells for tetramer staining (*see* Fig. 1 for example data showing an increase in NY-ESO-1 T cells during ipilimumab therapy).

3.4.3 Intracellular Cytokine Staining

1. For intracellular cytokine and staining detection of multiple parameters including expression of IFN-γ, IL-2, TNF-α, MIP-1β, and CD107a, harvest $2 \times 10e^6$ cultured T cells at Day 10 and resuspend in 1 mL 10 % PHS RPMI medium (*see* **Note 4**).
2. Restimulate the cells with the addition of corresponding peptides at 37 °C for the first 2 h and then in the presence of 5 μg/mL each of Brefeldin A and monensin for 4 h.
3. Add PE-Cy5-CD107a specific antibody (5 μL/mL or concentration 2.5 μg/mL) prior to stimulation. Harvest and wash the cells with 2 mL FACS buffer once.

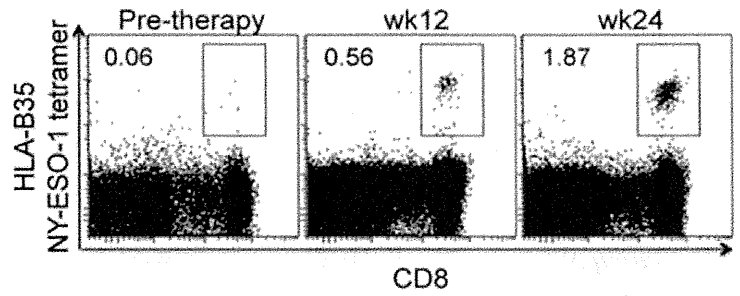

Fig. 1 Ipilimumab induced the expansion of NY-ESO-$1_{94\text{-}102}$ (MPFATPMEA) HLA/B*3501 tetramer + CD8+ T cells. PBMCs from both pre-therapy and post-therapy (week 12 and week 24) in a melanoma patient treated with 10 mg/kg of ipilimumab were cultured with NY-ESO-1 overlapping peptide for 10 days as described in Subheading 3.4. NY-ESO-$1_{94\text{-}102}$ (MPFATPMEA) HLA/B*3501 staining was performed on harvested T cells. A greater number of NY-ESO-$1_{94\text{-}102}$ (MPFATPMEA) HLA/B*3501 tetramer + CD8+ T cells were detected at week 12 and week 24 after ipilimumab treatment

4. Resuspend a total of $10e^6$ cells in FACS buffer and stain with the panel of antibodies for appropriate phenotypic cell surface markers and functional cytokine antibodies following fixation/permeabilization as described at Subheading 3.2.
5. Cells are analyzed by flow cytometry on a CYAN flow cytometer with Summit software to acquire the data. Perform further analysis on FlowJo software.

3.5 Myeloid-Derived Suppressor Cell Phenotype Staining

1. Wash thawed $5 \times 10e^5$ PBMCs from melanoma patients before and after treatment with 2 mL FACS buffer (*see* **Note 5**).
2. Add the following fluorochrome-conjugated antibodies: Lineage-specific antibodies (CD3/CD16/CD19/CD20/CD56) cocktail-FITC, and CD14-PerCP Cy5.5, CD11b-APC Cy7, CD33-PE-Cy7, and HLA-DR-ECD, and incubate at 4 °C for 20 min.
3. Include the appropriate fluorochrome-conjugated mouse IgG_1, IgG_k, IgG_{2a}, or IgG_{2bk} as isotype controls.
4. Detect the stained cells by using a CYAN flow cytometer. Use FlowJo software for all analysis (*see* **Note 5** and Fig. 2 for example gating strategy).

4 Notes

1. We optimize our phenotype flow staining for CD4 + $ICOS^{hi}$ T cells by performing each analysis in duplicate or triplicate and staining each PBMC sample for isotype control as well. In our experience, the frequency of CD4 + $ICOS^{hi}$ T cells is much higher in the tumor than in the peripheral blood. Therefore, we apply the gate of 0.5 % in the isotype control

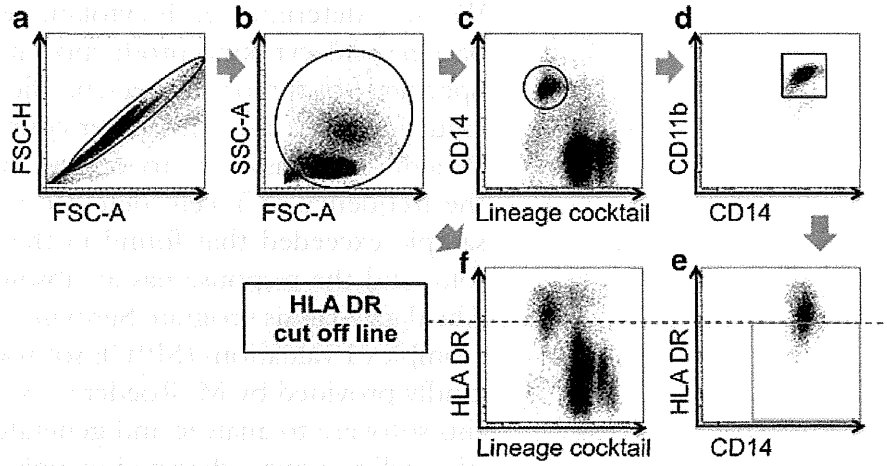

Fig. 2 MDSC gating strategy. MDSC are characterized as a CD14+CD11b+ population that is HLA-DR$^{low/-}$. After gating on single cells with forward scatter (FSC)-A and FSC-H selection (**a**), the myeloid population is gated based on side scatter (SSC) (**b**). Then, using our lineage cocktail (Subheading 3.5), we select CD14 positive cells that are lineage negative (**c**). The majority of these CD14 positive cells are CD11b positive (**d**). Finally, the selection of HLA-DR$^{low/-}$ cells in this population (**e**) is based upon the HLA-DR expression level on lymphocyte populations (lineage positive cells, **f**)

tube to select the real sample. We define a persistent increase in CD4+ICOS^{hi} expression as a ≥2-fold increase in % CD4+ICOS^{hi} expression at week 7 or 12 over baseline that is sustained at week 12.

2. We perform the analysis of serum samples by ELISA in a blinded fashion to the knowledge of clinical results. We test sera in 4× serial dilutions, starting from 1/100, for IgG reactivity against full-length NY-ESO-1. Using the control protein, DHFR, is essential to assess antibody specificity. Positive control sera with known reactivity on each plate are used to validate the assays. We usually do not detect antibody reactivity to DHFR in sera from patients with ipilimumab, assuring ourselves of its capabilities as a negative control. We also perform an extrapolation of antibody titers based on a pool of healthy donor sera with no reactivity to NY-ESO-1. We consider reciprocal titers positive if greater than 100.
3. We assess tumor antigen-specific T cell response by either tetramer or intracellular cytokine staining. To determine tetramer positive T-cell responses, we calculate the standard deviation of the pre-therapy replicate values taken at baseline. A tetramer T-cell response at any post-therapy time point is considered positive if it has a value ≥3 standard deviations than the mean value at baseline and has an absolute value of >0.1 %.
4. For intracellular cytokine staining, CD107a-specific antibody should be added to the culture prior to the stimulation.

We then determine each cytokine response by subtracting the background cytokine production in an unstimulated sample. Specificity of tumor antigen-specific T cell responses is considered significant if >3-fold over control (unpulsed target cells). Patients are considered to have an increase in T cell response if the frequency of T cells detected in at least one post-therapy sample exceeded that found in the baseline sample by three-fold, and the response has an absolute value of at least 0.1 %. The data analysis program Simplified Presentation of Incredibly Complex Evaluations (SPICE software, version 5.2.2) has been kindly provided by M. Roederer, NIH, Bethesda, MD. We use this software to analyze and generate graphical representations of T cell responses detected by polychromatic flow cytometry.

5. For MDSC analysis, we have found that peripheral blood samples should ideally be processed within 5–6 h from the patient's blood draw. In our experience, expression levels by mean fluorescence intensity (MFI) of HLA-DR molecules on CD14+CD11b+ cells increase with greater time in the blood collection tube. Consequently, the sensitivity of flow cytometry in detecting MDSC elevation is lost if the samples are processed after an overnight interval. The definition of MDSC (HLA-DR$^{low/-}$ on CD14+CD11b+ population) depends on the gating strategy. We draw the cut-off line between HLA-DR high and low—based on HLA-DR expression level on lymphocyte populations (lineage positive cells) within each sample, which are HLA-DR high and stable over time.

Acknowledgements

We would like to thank Erika Ritter and Teresa Rasalan for their critical review of the book chapter.

References

1. Hodi FS, O'Day SJ, McDermott DF et al (2010) Improved survival with ipilimumab in patients with metastatic melanoma. N Engl J Med 363:711–723
2. Robert C, Thomas L, Bondarenko I et al (2011) Ipilimumab plus dacarbazine for previously untreated metastatic melanoma. N Engl J Med 364:2517–2526
3. Topalian SL, Hodi FS, Brahmer JR et al (2012) Safety, activity, and immune correlates of anti-PD-1 antibody in cancer. N Engl J Med 366:2443–2454
4. Berman D, Wolchok J, Weber J et al (2009) Association of peripheral blood absolute lymphocyte count (ALC) and clinical activity in patients (pts) with advanced melanoma treated with ipilimumab. J Clin Oncol 27(suppl): 15s.3020 (abstr)
5. Ku GY, Yuan J, Page DB et al (2010) Single-institution experience with ipilimumab in advanced melanoma patients in the compassionate use setting: lymphocyte count after 2 doses correlates with survival. Cancer 116: 1767–1775
6. Postow M, Yuan J, Panageas K et al (2012) Evaluation of the absolute lymphocyte count as a biomarker for melanoma patients treated with the commercially available dose of ipilimumab (3mg/kg). J Clin Oncol 30(suppl):8575, abstr

7. Yang A, Kendle RF, Ginsberg BA et al (2010) CTLA-4 blockade with ipilimumab increases peripheral CD8+ T cells: correlation with clinical outcomes. J Clin Oncol 28(suppl):15s.2555, abstr
8. Hodi FS, Butler M, Oble DA et al (2008) Immunologic and clinical effects of antibody blockade of cytotoxic T lymphocyte-associated antigen 4 in previously vaccinated cancer patients. Proc Natl Acad Sci USA 105: 3005–3010
9. Hamid O, Schmidt H, Nissan A et al (2011) A prospective phase II trial exploring the association between tumor microenvironment biomarkers and clinical activity of ipilimumab in advanced melanoma. J Transl Med 9:204
10. Phan GQ, Yang JC, Sherry RM et al (2003) Cancer regression and autoimmunity induced by cytotoxic T lymphocyte-associated antigen 4 blockade in patients with metastatic melanoma. Proc Natl Acad Sci USA 100: 8372–8377
11. Attia P, Phan GQ, Maker AV et al (2005) Autoimmunity correlates with tumor regression in patients with metastatic melanoma treated with anti-cytotoxic T-lymphocyte antigen-4. J Clin Oncol 23:6043–6053
12. Maker AV, Phan GQ, Attia P et al (2005) Tumor regression and autoimmunity in patients treated with cytotoxic T lymphocyte-associated antigen 4 blockade and interleukin 2: a phase I/II study. Ann Surg Oncol 12:1005–1016
13. Maker AV, Yang JC, Sherry RM et al (2006) Intrapatient dose escalation of anti-CTLA-4 antibody in patients with metastatic melanoma. J Immunother 29:455–463
14. Comin-Anduix B, Lee Y, Jalil J et al (2008) Detailed analysis of immunologic effects of the cytotoxic T lymphocyte-associated antigen 4-blocking monoclonal antibody tremelimumab in peripheral blood of patients with melanoma. J Transl Med 6:22
15. Burmeister Y, Lischke T, Dahler AC et al (2008) ICOS controls the pool size of effector-memory and regulatory T cells. J Immunol 180:774–782
16. Liakou CI, Kamat A, Tang DN et al (2008) CTLA-4 blockade increases IFNgamma-producing CD4+ICOShi cells to shift the ratio of effector to regulatory T cells in cancer patients. Proc Natl Acad Sci USA 105: 14987–14992
17. Carthon BC, Wolchok JD, Yuan J et al (2010) Preoperative CTLA-4 blockade: tolerability and immune monitoring in the setting of a presurgical clinical trial. Clin Cancer Res 16(10):2861–2871
18. Wang W, Yu D, Sarnaik AA et al (2012) Biomarkers on melanoma patient T Cells associated with ipilimumab treatment. J Transl Med 10:146
19. Jungbluth AA, Chen YT, Stockert E et al (2001) Immunohistochemical analysis of NY-ESO-1 antigen expression in normal and malignant human tissues. Int J Cancer 92:856–860
20. Yuan J, Adamow M, Ginsberg BA et al (2011) Integrated NY-ESO-1 antibody and CD8+ T-cell responses correlate with clinical benefit in advanced melanoma patients treated with ipilimumab. Proc Natl Acad Sci U S A 108:16723–16728
21. Klein O, Ebert LM, Nicholaou T et al (2009) Melan-A-specific cytotoxic T cells are associated with tumor regression and autoimmunity following treatment with anti-CTLA-4. Clin Cancer Res 15:2507–2513
22. Weide B, Zelba H, Derhovanessian E et al (2012) Functional T cells targeting NY-ESO-1 or Melan-A are predictive for survival of patients with distant melanoma metastasis. J Clin Oncol 30:1835–1841
23. Filipazzi P, Valenti R, Huber V et al (2007) Identification of a new subset of myeloid suppressor cells in peripheral blood of melanoma patients with modulation by a granulocyte-macrophage colony-stimulation factor-based antitumor vaccine. J Clin Oncol 25: 2546–2553
24. Poschke I, Mougiakakos D, Hansson J et al (2010) Immature immunosuppressive CD14+HLA-DR-/low cells in melanoma patients are Stat3hi and overexpress CD80, CD83, and DC-sign. Cancer Res 70: 4335–4345
25. Postow MA, Callahan MK, Barker CA et al (2012) Immunologic correlates of the abscopal effect in a patient with melanoma. N Engl J Med 366:925–931
26. Kitano S, Postow M, Cortez C et al (2012) Myeloid-derived suppressor cell quantity prior to treatment with ipilimumab at 10mg/kg to predict for overall survival in patients with metastatic melanoma. J Clin Oncol 30(suppl):2518, abstr

BJ Cell

Biochem. J. (2014) 457, 313–322 (Printed in Great Britain) doi:10.1042/BJ20130827

online data

Identification of a binding element for the cytoplasmic regulator FROUNT in the membrane-proximal C-terminal region of chemokine receptors CCR2 and CCR5

Etsuko TODA*, Yuya TERASHIMA*[1], Kaori ESAKI†, Sosuke YOSHINAGA†, Minoru SUGIHARA‡, Yutaka KOFUKU§, Ichio SHIMADA§, Makiko SUWA‡‖, Shiro KANEGASAKI¶, Hiroaki TERASAWA† and Kouji MATSUSHIMA*

*Department of Molecular Preventive Medicine, Graduate School of Medicine, The University of Tokyo, Bunkyo-ku, Tokyo 113-0033, Japan
†Faculty of Life Sciences, Kumamoto University, 5-1 Oe-honmachi, Kumamoto 862-0973, Japan
‡National Institute of Advanced Industrial Science and Technology (AIST), Computational Biology Research Center (CBRC), Koutou-ku, Tokyo 135-0064, Japan
§Graduate School of Pharmaceutical Sciences, The University of Tokyo, Bunkyo-ku, Tokyo 113-0033, Japan
‖The Department of Chemistry and Biological Science, Aoyama Gakuin University, 5-10-1 Fuchinobe, Chuo-ku, Sagamihara-shi, Kanagawa 252-5258, Japan
¶YU-ECI Research Center for Medical Science, Yeungnam University, Gyeongsan 712-749, Korea

Chemokine receptors mediate the migration of leucocytes during inflammation. The cytoplasmic protein FROUNT binds to chemokine receptors CCR2 [chemokine (C-C motif) receptor 2] and CCR5, and amplifies chemotactic signals in leucocytes. Although the interaction between FROUNT and chemokine receptors is important for accurate chemotaxis, the interaction mechanism has not been elucidated. In the present study we identified a 16-amino-acid sequence responsible for high-affinity binding of FROUNT at the membrane-proximal C-terminal intracellular region of CCR2 (CCR2 Pro-C) by yeast two-hybrid analysis. Synthesized peptides corresponding to the CCR2 Pro-C sequence directly interacted with FROUNT *in vitro*. CCR2 Pro-C was predicted to form an amphipathic helix structure. Residues on the hydrophobic side are completely conserved among FROUNT-binding receptors, suggesting that the hydrophobic side is the responsible element for FROUNT binding. The L316T mutation to the hydrophobic side of the predicted helix decreased the affinity for FROUNT. Co-immunoprecipitation assays revealed that the CCR2 L316T mutation diminished the interaction between FROUNT and full-length CCR2 in cells. Furthermore, this mutation impaired the ability of the receptor to mediate chemotaxis. These findings provide the first description of the functional binding element in helix 8 of CCR2 for the cytosolic regulator FROUNT that mediates chemotactic signalling.

Key words: chemokine (C-C motif) receptor 2 (CCR2), chemotaxis, FROUNT, G-protein-coupled receptor (GPCR), helix 8.

INTRODUCTION

The chemokine receptor family comprises 19 GPCRs (G-protein-coupled receptors). The C-terminal intracellular domain of chemoattractant receptors is indispensable for chemotaxis [1,2] and the subsequent receptor endocytosis [3,4]. In particular, the membrane-proximal region of chemokine receptors seems to play an essential role in chemotaxis [5–10].

The cytoplasmic protein FNT [FROUNT; also known as NUP85 (nuclear pore complex protein Nup85)] directly interacts with the C-terminal intracellular domain of activated CCR2 [chemokine (C-C motif) receptor 2] and amplifies the chemokine-elicited PI3K (phosphoinositide 3-kinase)–Rac–lamellipodium protrusion cascade, promoting subsequent chemotaxis. If the interaction between FNT and CCR2 is blocked, the chemotactic response is prevented [11], suggesting that the interaction between FNT and CCR2 plays a crucial role in CCR2-mediated chemotaxis.

We reported previously that FNT is a common regulator of CCR2 and another chemokine receptor CCR5 [12]. Although the functions of CCR2 and CCR5 differ owing to different chemokine usage, these receptors mediate the migration and infiltration of monocyte/macrophages and are involved in the pathogenesis and progression of cancer and inflammatory diseases, such as arteriosclerosis, multiple sclerosis and graft versus host disease [13–16]. Thus the interaction between CCR2/CCR5 and FNT is a promising drug target for inflammatory diseases; however, the molecular mechanism underlying the binding of FNT to CCR2/CCR5 has not been elucidated.

To investigate the molecular mechanism of the interaction between CCR2 and FNT, in the present study we have identified a short sequence in the membrane-proximal C-terminal region of CCR2 (CCR2 Pro-C) responsible for efficient binding to FNT. This sequence is predicted to form a helical structure, and we have identified residues (Leu^{316} and His^{323}) crucial for FNT binding on the hydrophobic side of the predicted helix. Interestingly, the residues on the hydrophobic side of CCR2 are identical to those of the other chemokine receptor CCR5 to which FNT binds. Thus in the present study we define the hydrophobic side of a 16-amino-acid putative helix of CCR2/CCR5 Pro-C as an element for high-affinity binding to FNT. Furthermore, co-immunoprecipitation assays revealed that a low-affinity L316T mutation in this binding element impairs the interaction between full-length CCR2 and FNT in cultured cells. This low-affinity mutation correlated with the impaired chemotaxis mediated by CCR2.

EXPERIMENTAL

Proteins and peptides

Full-length human FNT was expressed in *Escherichia coli* cells as a soluble protein, as described by Esaki et al. [17]. The C-terminal

Abbreviations: CCR, chemokine (C-C motif) receptor; CXCR, chemokine (C-X-C motif) receptor; Em, emission; FNT, FROUNT; GPCR, G-protein-coupled receptor; HEK, human embryonic kidney; HTRF, homogeneous time-resolved fluorescence; LASP-1, LIM and Src homology 3 domain protein-1; ONPG, *o*-nitrophenyl β-D-galactopyranoside; PI3K, phosphoinositide 3-kinase; SPR, surface plasmon resonance; Y2H, yeast two-hybrid.

[1] To whom correspondence should be addressed (email tera@m.u-tokyo.ac.jp).

region of FNT (FNT-C) was fused to a GST tag and GST–FNT-C was expressed in *E. coli* BL21 cells (Merck Millipore) as a soluble protein. The cells were lysed, and the GST–FNT-C protein was purified using a glutathione–Sepharose 4B column (GE Healthcare). For preparation of unlabelled FNT-C, GST was excised from FNT-C by thrombin protease in the column. FNT-C was further purified using a Q Sepharose Fast Flow column, followed by Superdex 200 gel filtration chromatography (GE Healthcare). Peptides corresponding to the FNT-binding region of CCR2 and CCR5 or CXCR4 [chemokine (C-X-C motif) receptor 4; EKFRRYLSVFFRKHIT, EKFRNYLLVFFQKHIA or AKFKTSAQHALTSVSR respectively], and other mutants (L316T, EKFRRYTSVFFRKHIT and H323Y, EKFRRYLSVFFRKYIT; underlined residue indicates the mutation) were custom synthesized (Hayashi Kasei). In some experiments, peptides biotinylated at the N-terminal side were used.

Yeast two-hybrid system

Deletion mutants were generated from cDNAs encoding the C-terminal domain of CCR2 and subcloned into pAS2-1 GAL4-BD (Clontech). These clones and the pACT GAL4-AD vector (Clontech) containing a cDNA encoding amino acids 500–656 of human FNT were co-transfected into yeast Y190 cells using a lithium acetate protocol. Double-positive clones were selected by growth in selection medium lacking tryptophan (T) and leucine (L) (TL medium). Interactions between FNT and each deletion mutant of CCR2 in yeast cells were tested for histidine (H) auxotrophy (TLH medium) and β-galactosidase activity using a filter lift assay. A semi-quantitative liquid β-galactosidase assay using ONPG (*o*-nitrophenyl β-D-galactopyranoside) as a substrate was performed according to the protocol described for the MATCHMAKER System-2 (Clontech).

SPR analysis

The interactions between FNT and the CCR2 Pro-C peptide or various mutants of this peptide were analysed by SPR (surface plasmon resonance) using Biacore X and Biacore2000 instruments (GE Healthcare). FNT protein was immobilized on the CM5 sensor chip, and various concentrations of the CCR2 Pro-C peptide in HBS-EP buffer (GE Healthcare) were applied to the sensor chip at a flow rate of 20 μl per min and then washed out with HBS-EP buffer. For the experiment determining the binding ability of CCR5 Pro-C to FNT, CCR5 Pro-C peptide with two lysine residues added to the C-terminus was used. For the other experiments, the Pro-C peptide was immobilized on the CM5 sensor chip and FNT protein was applied to the sensor chip at the same flow rate. RUs (resonance units) were measured during the binding and washing periods, and the binding kinetics were analysed using BIAevaluation software version 3.0. Kinetic constants were obtained from the association and dissociation curves generated from different concentrations of analyte by using the 1:1 Langmuir binding model ($A + B \leftrightarrow AB$) available in the software. This model was found to fit the data very well when GST–FNT (Figure 2B), but not the CCR2 Pro-C peptide, was used as the analyte (Figure 2A). Use of a more complex binding model did not give a better fit of the data. All binding curves were corrected for background by subtraction of the reference flow cells.

HTRF-based binding assay

The HTRF (homogeneous time-resolved fluorescence) assay was performed in white 384-well low-volume microplates (Corning Coaster). To achieve the composition of the final reaction solution, 5 nM GST-fused FNT-C, 250 nM biotinylated Pro-C peptide, 2.6 ng of anti-GST antibody labelled with Europium Cryptate and 12.5 ng of high-grade XL665-conjugated streptavidin were mixed in HTRF buffer [10 mM Hepes (pH 7.4), 0.2 M potassium fluoride, 10 mM NaCl, 0.1 % Tween 20 and 0.5 % BSA]. As a negative control, a biotinylated peptide corresponding to the CXCR4 sequence was used. HTRF signals were measured at room temperature (25°C) using an Envision instrument (PerkinElmer) at 620 and 665 nm Em (emission) wavelengths. The results are expressed as a Em_{665nm}/Em_{620nm} ratio or Delta F calculated by eqn (1):

$$\text{Delta F} = \frac{\text{sample ratio} - \text{ratio}_{neg}}{\text{ratio}_{neg}} \times 100 \quad (1)$$

In the competition assay, unlabelled FNT-C or full-length FNT and unrelated recombinant protein as a control were added at the indicated concentrations into the HTRF reaction mixture containing 5 nM GST–FNT and 250 nM CCR2 Pro-C peptide.

Cluster analysis of GPCRs

We retrieved 1272 vertebrate GPCR sequences from the SEVENS database (http://sevens.cbrc.jp) [17a] and compared them with UniProt/Swiss-Prot. The regions of transmembrane helices (TMH1–TMH7) and loop regions of these sequences were determined on the basis of the available crystal structures of bovine rhodopsin, adrenergic receptors and the adenosine receptor, to which multiple sequence alignments of the selected sequences were assigned with avoidance of gaps in the transmembrane domains. The multiple sequence alignment was modified by manual curation. The detailed conditions of the sequence comparison and detailed principles of the multiple structural alignment are described previously [18]. In the present analysis, 16 residues corresponding to positions 310–325 of the CCR2 sequence are defined as the Pro-C region. We selected the corresponding regions of 179 human GPCRs, including 19 chemokine receptors {CCR1–CCR10, CCRL1 (CCR-like 1), CXCR1–CXCR6, CX3CR1 [chemokine (C-X3-C motif) receptor 1] and XCR1 [chemokine (C motif) receptor 1]}, on the basis of the alignment. These amino acid sequences were translated to feature vectors with the following physico-chemical elements: molecular mass [19], charge, p*K* value [20], hydrophobicity [21] and number of hydrogen bonds [22] for each amino acid. The vectors of the short Pro-C region sequences and the full-length sequences were then analysed by a clustering method (Ward method). This methodology is adequate to link sequences that have similar physico-chemical properties even though they have no sequence similarity.

Semi-random mutagenesis and selection

To generate a mutational library of the CCR2 Pro-C region, semi-random mutagenesis of the pAS2-1 CCR2 vector was performed by following the guidelines of Sawano and Miyawaki [23] with the exception of the oligonucleotides TR448 (35-mer), 5′-CATG-GAGGCCGAATTCNNGAAGTTCAGAAGGTATC-3′; TR449 (34-mer), 5′-GGAGGCCGAATTCGAGNNGTTCAGAAGGTA-TCTC-3; TR450 (34-mer), 5′-GGCCGAATTCGAGAAGNN-CAGAAGGTATCTCTCG-3; TR451 (34-mer), 5′-CGAATTCG-AGAAGTTCNNAAGGTATCTCTCGGTG-3′; TR452 (33-mer), 5′-GAGAAGTTCAGAAGGNNTCTCTCGGTGTTCTTC-3′; TR453 (33-mer), 5′-GAAGTTCAGAAGGTATNNCTCGGTG-

TTCTTCCG-3′; TR454 (32-mer), 5′-GGTATCTCTCGGTGNN-CTTCCGAAAGCACATC-3′; TR455 (31-mer), 5′-GTATCTCT-CGGTGTTCNNCCGAAAGCACATC-3′; TR456 (32-mer), 5′-CTCGGTGTTCTTCCGANNGCACATCACCAAGCG-3′; and TR457 (35-mer), 5′-CGGTGTTCTTCCGAAAGNNCATCACC-AAGCG-3′ that were used to generate the semi-randomized mutants. In the above oligonucleotide sequences 'N' designates the inclusion of equimolar concentrations of all of the nucleotides during oligonucleotide synthesis. More than 100 mutants were sequenced and 78 different clones were picked up. FNT-binding affinity was tested by an ONPG assay in yeast cells. High- and low-affinity mutated CCR2 Pro-C peptides were synthesized and selected by both SPR analysis and HTRF assay.

Co-immunoprecipitation assay

Human FROUNT cDNA (corresponding to amino acids 23–656) fused to EGFP, and human CCR2 (pcMGS-CCR2) or low-affinity mutant human CCR2 (pcMGS-CCR2-L316T) cDNA were co-transfected into HEK (human embryonic kidney)-293 cells with the Lipofectamine® reagent (Invitrogen). Transfection efficiency was confirmed by GFP fluorescence and CCR2 staining by an anti-(human phycoerythrin-conjugated CCR2) antibody (R&D Laboratories) using a Gallios flow cytometer (Beckman Coulter). More than 90 % of cells were positive for CCR2 expression. These cells were stimulated with CCL2 (Peprotech) for 5 min and then lysed in a detergent buffer containing 50 mmol/l Tris/HCl buffer (pH 7.6), 150 mmol/l NaCl, 1 % Nonidet P40, 0.5 % sodium deoxycholate and Protease Inhibitor cocktail (Nakarai). Samples were then centrifuged at 10 000 *g* for 10 min at 4 °C. The soluble fraction was incubated at 4 °C with a mouse anti-FLAG (M2) antibody coupled to Dynabeads® M-270 epoxy (Invitrogen) for 30 min. Immunoprecipitates were eluted and subjected to SDS/PAGE (4–12% gel), transferred on to PVDF membranes and stained with anti-EGFP (Clontech) or anti-FLAG antibody (Invitrogen).

Chemotaxis assay

Human Jurkat cells were maintained in RPMI 1640 medium supplemented with 10 % FBS. Human CCR2 or CCR2-L316T (a low-affinity mutant) and the EGFP vector, as a marker for gene expression, were transiently co-transfected into Jurkat cells using a Nucleofector device (Amaxa) and a Nucleofection kit V according to the manufacturer's instructions. At 16 h after nucleofection, living cells at a density of 10^6 cells/ml were placed into the upper chamber of a 96-well chemotaxis chamber (Neuroprobe) with a polycarbonate filter (5-μm pore size). After incubation at 37 °C for 120 min, EGFP-positive cells that had migrated to the lower chamber containing medium or CCL2 (Peprotech) were counted under a fluorescence microscope.

RESULTS

A 16-amino-acid sequence in the membrane-proximal region of the C-terminal cytoplasmic tail of CCR2 is responsible for efficient binding to FNT

The cytoplasmic chemotaxis regulator FNT has been identified as a molecule that binds to the C-terminal region of CCR2 in a Y2H (yeast two-hybrid) system [11]. To pinpoint the region needed for FNT binding, we examined a series of C-terminal-truncation mutants of CCR2 for their ability to bind FNT in Y2H assays (Figure 1A). The results are summarized in Figure 1(B). Truncation of the distal C-terminal region (amino acids 329–360) of CCR2 maintained the interaction with FNT (clone CCR2-0 in Figure 1B and [11]). A further 5-amino-acid deletion at the C-terminal end (Figure 1B, clones CCR2-1–CCR2-5) did not reduce the ability to bind FNT. Interestingly, truncation of a further three amino acids from 309–328 at the C-terminal end (Figure 1B, clone CCR2-3) led to increased binding ability in the β-galactosidase assay, whereas a further deletion of three amino acids (Figure 1B, CCR2-6) led to decreased FNT binding. Regarding the N-terminal end, deletion of more than two amino acids (Figure 1B, CCR2-9 and CCR2-13) completely diminished the ability to bind FNT. A semi-quantitative ONPG assay revealed that the most potent binding ability was exhibited by clone CCR2-12 (Figure 1C). Thus a 16-amino-acid region corresponding to residues 310–325 of CCR2 (CCR2 Pro-C) was defined as the high-affinity region for FNT.

The Pro-C sequence of CCR2 alone directly interacts with FNT

To confirm whether the identified region directly binds to FNT *in vitro*, a 16-amino-acid peptide corresponding to the Pro-C high-affinity region for FNT was synthesized and assessed for binding to the FNT protein by SPR. The CCR2 Pro-C peptide showed a dose-dependent response towards the C-terminal CCR2-binding region of FNT tagged with GST (GST–FNT-C) immobilized on a sensorchip, whereas the control (CXCR4 Pro-C) did not (Figure 2A). A reverse assay was performed in which the CCR2 Pro-C peptide was immobilized along with the CXCR4 peptide as a reference. The GST-fused FNT protein (but not GST alone) gave a dose-dependent binding response to the CCR2 Pro-C peptide ($K_d = 5.3$ μM) (Figure 2B).

We further tested the interaction between the CCR2 Pro-C and FNT in solution by using a HTRF assay. The interaction was detected by using an indirect 'cassette format', in which the interaction between GST–FNT-C and the biotinylated CCR2 Pro-C peptide was detected by an anti-tag donor/acceptor pair, namely cryptate-labelled anti-GST antibody and a streptavidin-XL665 conjugate respectively. The CCR2 Pro-C peptide biotinylated at the N-terminal end used in this assay showed FNT binding comparable with that of unlabelled peptides in the SPR analysis (results not shown). In this assay, when the CCR2 Pro-C peptide was mixed with GST–FNT-C protein, but not with GST alone, a FRET signal was observed (Figure 2C). By contrast, no signal was observed when CXCR4 Pro-C was mixed with GST–FNT-C (Figure 2C). The FRET signal was observed within a few minutes when the CCR2 Pro-C peptide was mixed with GST–FNT in a dose-dependent manner (Figure 2D). The specific interaction of FNT and CCR2 Pro-C was confirmed by a competition assay (Figure 2E). An unlabelled FNT fragment (FNT-C) or full-length FNT inhibited this interaction dose-dependently, whereas the control protein did not.

Clustering analysis of various human GPCRs by Pro-C region highlights conservation among FNT-binding receptors

Identification of the 16-amino-acid short sequence for FNT binding in CCR2 prompted us to look for conservation of this sequence among known GPCRs. We generated dendrograms based on feature vectors of the full-length amino acid sequence and the 16-amino-acid Pro-C region (see the Supplementary Online Data at http://www.biochemj.org/bj/457/bj4570313add.htm). The dendrogram generated from feature vectors of the full-length sequences gave the expected clustering of receptor families; thus the chemokine receptor family (19 receptors) was found

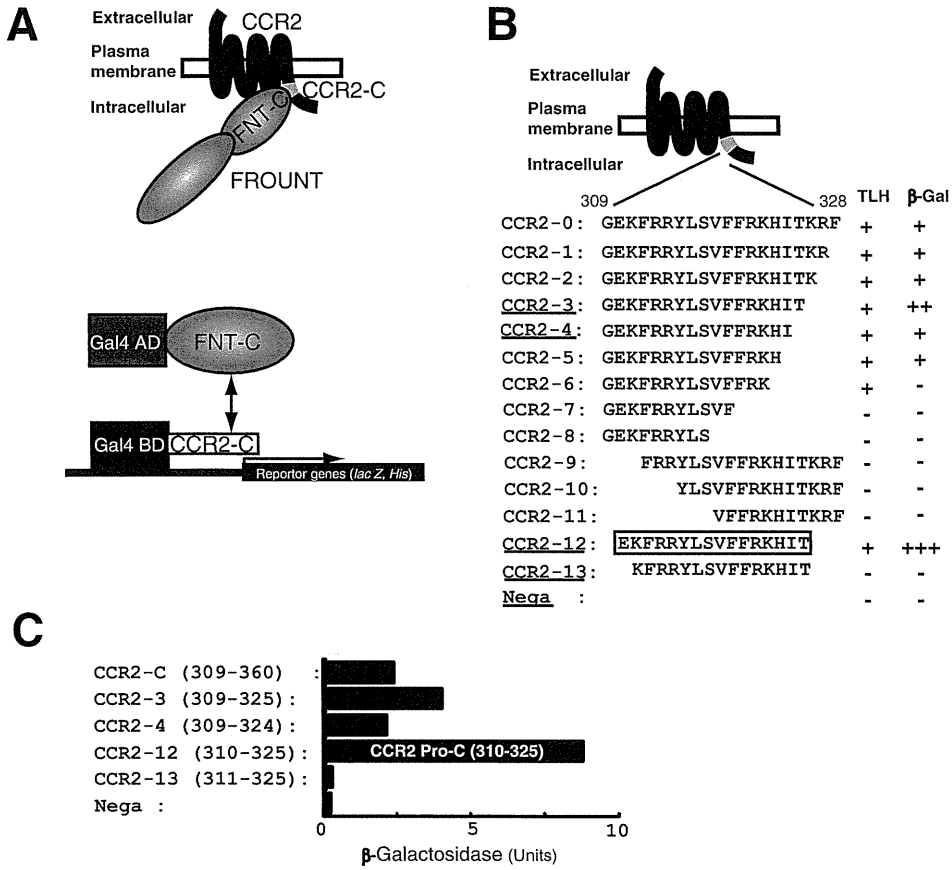

Figure 1 Identification of a short sequence with a high affinity for FNT at the membrane-proximal C-terminal region of CCR2

(**A**) To pinpoint the region in the C-terminal domain of CCR2 responsible for FNT binding, sequential truncation mutants of the C-terminal domain of CCR2 were generated and assessed for their ability to bind FNT by Y2H analysis. (**B**) The FNT-binding ability of each truncation mutant was assessed by expression of a reporter gene measured using auxotrophy (TLH) and a colorimetric β-galactoside (β-gal) assays. (**C**) The binding ability of various lengths of the truncation mutants (underlined in **B**) was quantified by an ONPG assay. A 16-amino-acid region corresponding to residues 310–325 of CCR2 (CCR2 Pro-C; membrane-proximal C-terminal intracellular region) was defined as the high-affinity region for FNT (boxed area in **B**). Nega, control vector.

in the same clade. In the dendrogram generated from the short feature vectors of the Pro-C region, the topology of the dendrogram changed markedly, with the chemokine receptor family interspersed among the clades. Notably, however, CCR2 and CCR5 (to which FNT binds) were located proximally, whereas CXCR4 (to which FNT does not bind) appeared on a distant branch. These results indicate that CCR2 and CCR5 are the most homologous in the Pro-C sequence among all 179 of the examined GPCRs.

The Pro-C region of CCR2 may form an amphipathic helix and residues on the hydrophobic side of the predicted helix are responsible for FNT binding

To identify the key residues in CCR2 Pro-C responsible for the interaction with FNT, CCR2 Pro-C mutants were semi-randomly generated in a Y2H vector (Figure 3A), and 78 clones were tested for their ability to bind FNT using an ONPG assay (Figure 3B). Subsequently, those peptides with an amino acid mutation affecting FNT binding in the Y2H assay were synthesized and their binding strength was verified by SPR. Among the mutant CCR2 Pro-C peptides tested, substitution of Leu^{316} with a threonine residue (CCR2 Pro-C L316T) resulted in a marked reduction in binding to the immobilized FNT protein (Figure 4A, left-hand panel), whereas substitution of His^{323} with a tyrosine residue (CCR2 Pro-C H323Y) markedly increased the binding response to FNT (Figure 4A, right-hand panel).

Most GPCRs have an amphipathic helical structure, located proximal to the seventh transmembrane domain. CCR2 is also predicted to have a helical structure in this region, as revealed by the PSIPRED protein structure prediction server (http://bioinf.cs.ucl.ac.uk/psipred/) [23a] (Figure 4B). The 16-amino-acid Pro-C region identified for FNT binding lies completely within this helical region. Helical wheel projection revealed that CCR2 Pro-C contains a grey-coloured hydrophobic cluster on one face (Figure 4C, middle panel), suggesting that CCR2 Pro-C forms an amphipathic α-helical structure. Interestingly, both of the residues implicated in FNT binding by Y2H and SPR analysis are located in the hydrophobic cluster of CCR2 Pro-C (Figure 4C).

An HTRF assay also revealed the increased binding of the H323Y mutant and the decreased binding of the L316T mutant to the FNT C-terminal region (Figure 4D). Consistent with its binding affinity for FNT, unlabelled high-affinity mutant H323Y peptide competed more efficiently than the wild-type sequence with the labelled wild-type CCR2 pro-C peptide for FNT binding, whereas the low-affinity mutant peptide L316T failed to compete (Figure 4E). Taken together, these results indicate that the hydrophobic side of the 16-amino-acid CCR2 Pro-C helix is responsible for binding to FNT.

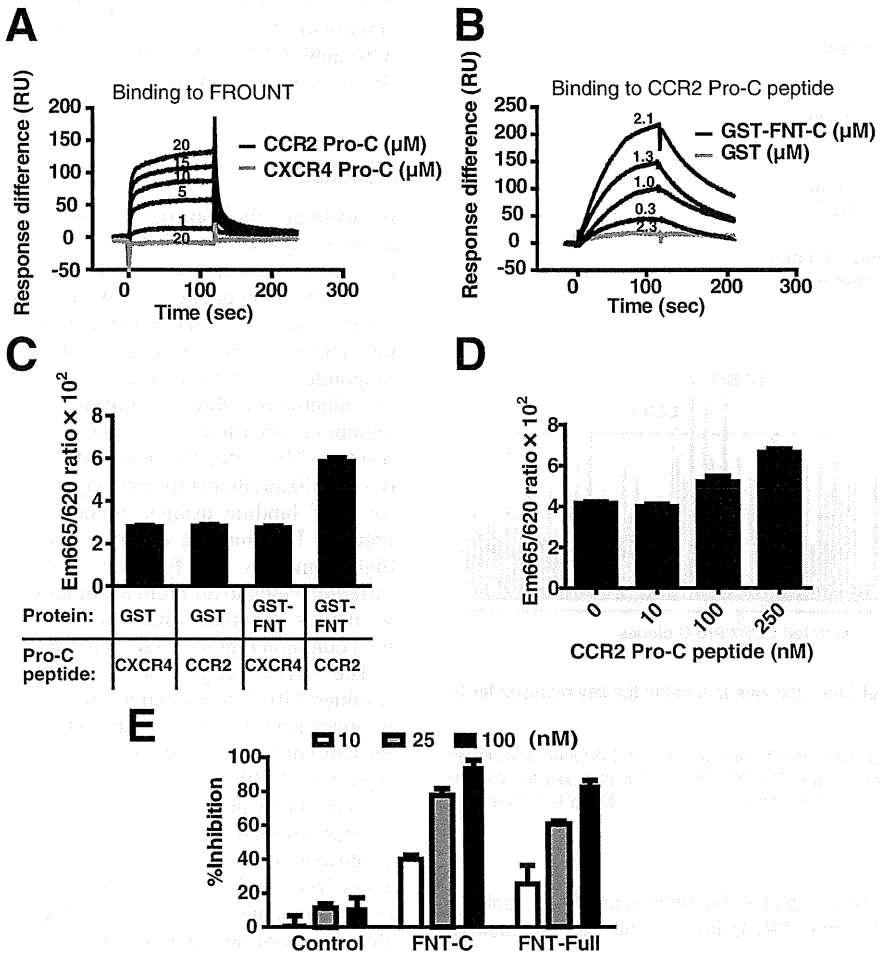

Figure 2 Interaction between FNT and the 16-amino-acid CCR2 ProC peptide

The synthetic CCR2 peptide corresponding to the FNT-binding domain (16-amino-acid sequence of CCR2 Pro-C) determined in Figure 1 was assessed for binding to the FNT protein. (**A**) SPR sensorgrams of CCR2 Pro-C peptide binding to the immobilized GST-fused FNT C-terminal fragment (FNT-C) are shown. A peptide derived from the CXCR4 sequence corresponding to the location of CCR2 Pro-C was used as a control (CXCR4 Pro-C, grey line). (**B**) SPR sensorgrams of GST-fused FNT-C (black line) and GST protein (grey line) binding to immobilized CCR2 Pro-C peptide. (**C**) The ability of the CCR2 Pro-C peptide to bind to FNT was examined by a HTRF assay using an indirect 'cassette format', in which the interaction between GST-fused FNT-C and the biotinylated CCR2 Pro-C peptide was detected by an anti-tag donor/acceptor pair, namely cryptate-labelled anti-GST antibodies and a streptavidin-XL665 conjugate respectively. GST protein and the biotinylated CXCR4 Pro-C peptide were used as controls. Data at 30 min after mixing are shown. (**D**) Interaction between CCR2 Pro-C and FNT at various concentrations of CCR2 Pro-C peptide. Data at 5 min after mixing are shown. (**E**) HTRF competition assay using unlabelled fragment (FNT-C) or full-length (FNT-Full) FNT protein. The competitors were added to the HTRF reaction mixture between GST-fused FNT-C and CCR2 Pro-C as described in (**C**). The percentage inhibition of the FNT–CCR2 Pro-C interaction caused by the addition of each competitor was calculated relative to the signal obtained from a negative control. Results are means ± S.D.

Residues on the hydrophobic side of the helix-prone Pro-C region are completely conserved among two FNT-binding receptors

FNT also binds to another chemokine receptor, CCR5, to promote the directional migration of cells [12]. To gain further insight into the key residues for binding to FNT, we compared the properties of the Pro-C 16-amino-acid sequence of CCR2 with that of CCR5. The C-terminal regions of CCR2 and CCR5 possess high similarity. Regarding the Pro-C 16-amino-acid sequence of CCR2 identified as FNT binding in the Y2H assay, the corresponding sequence of CCR5 is identical except for four amino acids. Helical wheel analysis showed that CCR5 Pro-C also exhibits an amphipathic α-helical structure (Figure 5A, middle panel). Note that this region of CXCR4, which does not interact with FNT in either the Y2H or SPR analysis, does not contain the highly hydrophobic cluster seen in CCR2 (Figure 5A, bottom panel). The four different amino acids in CCR5 are all located on the side opposite to the hydrophobic cluster, whereas the residues comprising the hydrophobic side are identical to those of CCR2 Pro-C (Figure 5A, top panel). As expected from the above observation, the CCR5 Pro-C peptide bound efficiently to FNT in the SPR analysis (Figure 5B). We also tested the ability of the 16-amino-acid peptide of CCR5 to bind to FNT in an HTRF assay (Figure 5C). The biotinylated 16-amino-acid CCR5 peptide gave a response comparable with that of CCR2 when mixed with FNT. Furthermore, the competition assay shows that the unlabelled CCR5 Pro-C peptide, but not the CXCR4 Pro-C peptide, inhibited the interaction between the biotinylated CCR2 Pro-C peptide and FNT (Figure 5D). These results indicate that the common residues on the hydrophobic side of CCR2 and CCR5 Pro-C define the receptors' ability to bind to FNT.

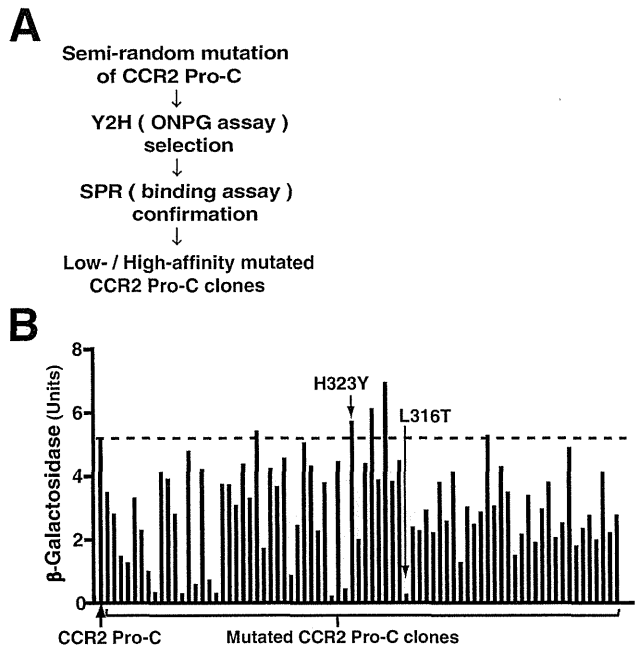

Figure 3 Generation of Pro-C mutants to identify the key residues for the interaction with FNT

(**A**) Experimental procedure to assess the FNT-binding affinity of CCR2 Pro-C point mutants generated by random mutagenesis using PCR. (**B**) CCR2 Pro-C mutants were tested for their ability to bind FNT by a high-throughput ONPG assay in yeast cells. Mutant H323Y and mutant L316T are indicated by arrows.

Mutation in the hydrophobic side of the helix-prone Pro-C region impairs the ability of whole CCR2 to interact with FNT and mediate chemotaxis

To confirm the role of the element of CCR2 identified for FNT binding in the context of the whole receptor molecule, we compared the FNT binding ability of full-length wild-type CCR2 and full-length CCR2 with a mutation corresponding to the low-affinity mutant of the Pro-C peptide identified by SPR and HTRF (CCR2-L316T) in a co-immunoprecipitation analysis. cDNA encoding human CCR2 or CCR2-L316T tagged with FLAG, and cDNA encoding EGFP-fused FNT were co-transfected into HEK-293 cells, and these receptors were expressed on the cell surface in equal amounts (Figure 6A). Immunoprecipitation was performed using the anti-FLAG antibody (Figure 6B), and co-immunoprecipitation of the FNT protein with CCR2 was detected by the anti-EGFP antibody (Figure 6C). Less FNT was co-immunoprecipitated with the CCR2-L316T mutant (Figures 6C and 6D), even though immunoprecipitation of the mutant receptor was equal to that of the wild-type receptor (Figure 6B). These results demonstrate that the key residue for binding to FNT identified *in vitro*, Leu^{316} in CCR2 Pro-C, has a crucial role in the full-length CCR2–FNT interaction in cells. Next, we evaluated the effect of the L316T mutation on CCR2-mediated chemotaxis. Wild-type CCR2 or the CCR2-L316T expression vector used in Figures 6(A)–6(D) was transfected into human Jurkat T-cells, which express endogenous FNT, but not CCR2. CCR2-transfected cells, but not cells transfected with control vector, exhibited chemotactic activity toward CCL2 (results not shown). Although CCR2-L316T was expressed on the cell surface comparably with the wild-type CCR2, chemotactic activity was significantly diminished in cells transfected with CCR2-L316 (Figure 6E). These results demonstrate that the key residue for binding to FNT identified *in vitro*, Leu^{316}, has a crucial role in the full-length CCR2–FNT interaction in cells and in the receptor's ability to mediate chemotaxis.

DISCUSSION

Intracellular chemotactic signals mediated via the chemokine receptors CCR2 and CCR5 are positively modulated by their interaction with the cytosolic regulator FNT. FNT amplifies the chemokine-elicited PI3K–Rac–lamellipodium protrusion cascade; however, the molecular mechanism underlying this interaction has not been elucidated. In the present study, we pinpointed the receptor region responsible for binding to FNT and identified a short high-affinity amino acid sequence in the membrane-proximal C-terminal region of CCR2 (CCR2 Pro-C; residues 310–325). We demonstrated that the hydrophobic side of the helix predicted for this sequence is the element responsible for FNT binding using a mutational study and a comparison between FNT-binding and non-binding receptors. Despite their high homology, the function of these receptors seems to be different owing to different chemokine usage. In the present study, we propose that these different chemokine receptors are regulated by a common regulator via a common binding element.

The Y2H assay of a series of deletion mutants revealed that residues 310–325 exhibited a more efficient binding than either a longer peptide or the entire cytoplasmic tail (Figure 1C). The present study clearly shows the potential of this 16-amino-acid region of CCR2/CCR5 to interact with FNT (Figures 2 and 5). The direct interaction between a 16-amino-acid synthesized peptide, corresponding to CCR2 Pro-C, and the FNT protein was confirmed by two different approaches, SPR analysis and HTRF assay. The affinity of the interaction between FNT and CCR2 was estimated at approximately 5 μM (Figure 2B). The specificity of the interaction was demonstrated by competition with either the unlabelled full-length or the C-terminal domain of FNT, and by the lack of competition with the control protein (Figure 2E).

Furthermore, we confirmed the role of the identified FNT-binding element of CCR2 in the context of the whole receptor molecule (Figure 6). The L316T mutation, which impaired the interaction of CCR2 pro-C with FNT in Y2H, SPR and HTRF analyses, also impaired the ability of the whole CCR2 molecule to interact with FNT in human cultured cells. Moreover, we revealed that the mutation in the FNT-binding element of CCR2 dramatically impaired the receptor's ability to mediate cellular chemotaxis.

Identification of a short sequence for FNT binding in CCR2 enabled us to propose a new grouping of GPCRs on the basis of the 16-amino-acid sequence at the membrane-proximal C-terminal region corresponding to the FNT-binding region of CCR2 (see the Supplementary Online Data). Chemokine receptors are interspersed in the dendrogram based on this sequence. Nevertheless, no other GPCRs share more homology in the Pro-C region than CCR2 and CCR5 despite the shortness of the region. Intriguingly, this clustering analysis suggests that other neighbouring pairs of receptors might share different Pro-C-binding molecules.

There are several reports on cytoplasmic molecules binding via the Pro-C region. For example, in the case of CXCR2, a chemokine receptor expressed on neutrophils, LASP-1 [LIM and SH3 (Src homology 3) domain protein-1] has been reported to bind to the C-terminal region of the receptor [24]. The residues responsible for LASP-1 binding are located in the region corresponding to the 16-amino-acid FNT-binding site of

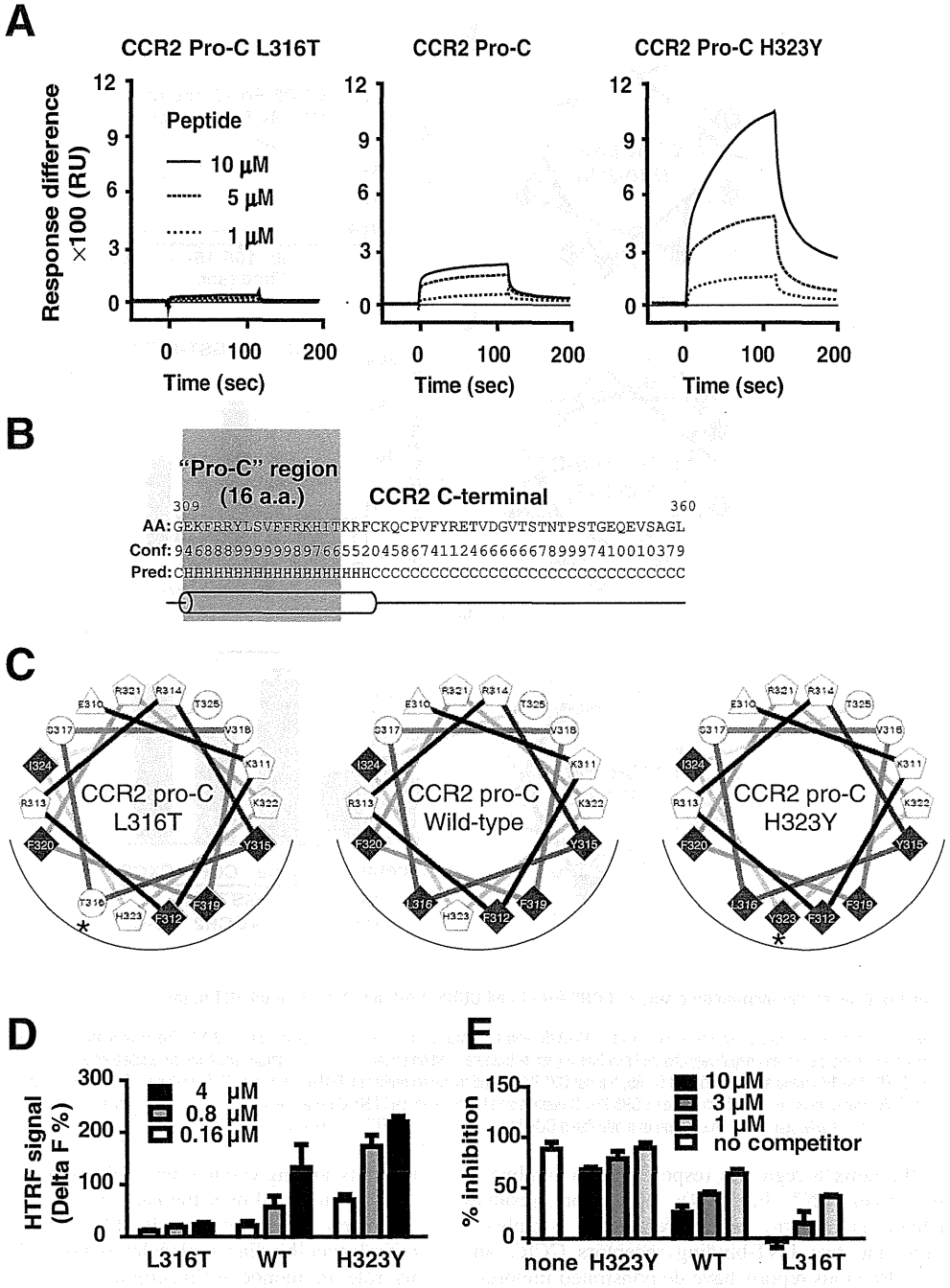

Figure 4 Binding of the mutated CCR2 Pro-C to FNT and role of the amphipathic helical structure in CCR2 Pro-C on FNT binding

(**A**) SPR sensorgrams of synthetic peptides of native and mutated CCR2 Pro-C at the indicated concentration binding to immobilized FNT protein. (**B**) The confidence rate (Conf) for a helical secondary structure (0 = low and 9 = high) of the C-terminal region of CCR2 was calculated by the PSIPRED protein structure prediction server. The shaded area indicates the frame identified as the FNT-binding region. (**C**) Helical wheel projections of Pro-C sequences with low FNT affinity (L316T, left-hand panel), high FNT affinity (H323Y, right-hand panel) and native sequence (middle panel) (http://rzlab.ucr.edu/scripts/wheel/wheel.cgi). The hydrophobic residues are grey-coloured diamonds, hydrophilic residues are white circles, potentially negatively charged residues are white triangles and potentially positively residues charged are white pentagons. The asterisk indicates the mutated amino acid. (**D**) Interaction signals (Delta F) of native or the mutated CCR2 Pro-C biotinylated peptide with FNT in HTRF (means ± S.D.). (**E**) Effect of native or mutated CCR2 Pro-C unlabelled peptide added as a competitor in the interaction of biotinylated native CCR2 Pro-C peptide with FNT in HTRF (means ± S.D.).

CCR2/CCR5, but are not identical to those responsible for FNT binding, indicating that the sequence of this region defines the characteristics for binding cytoplasmic regulatory molecules.

Chemokine receptors are GPCRs containing seven transmembrane domains. Most structurally characterized GPCRs have helical structures in the membrane-proximal C-terminal region (helix 8). Indeed, the presence of helix 8 has been reported in a crystal structure of CCR5 [25]. The FNT-binding region of CCR2/CCR5 identified in the present study is located in the so-called helix 8 region. Our studies demonstrated that the

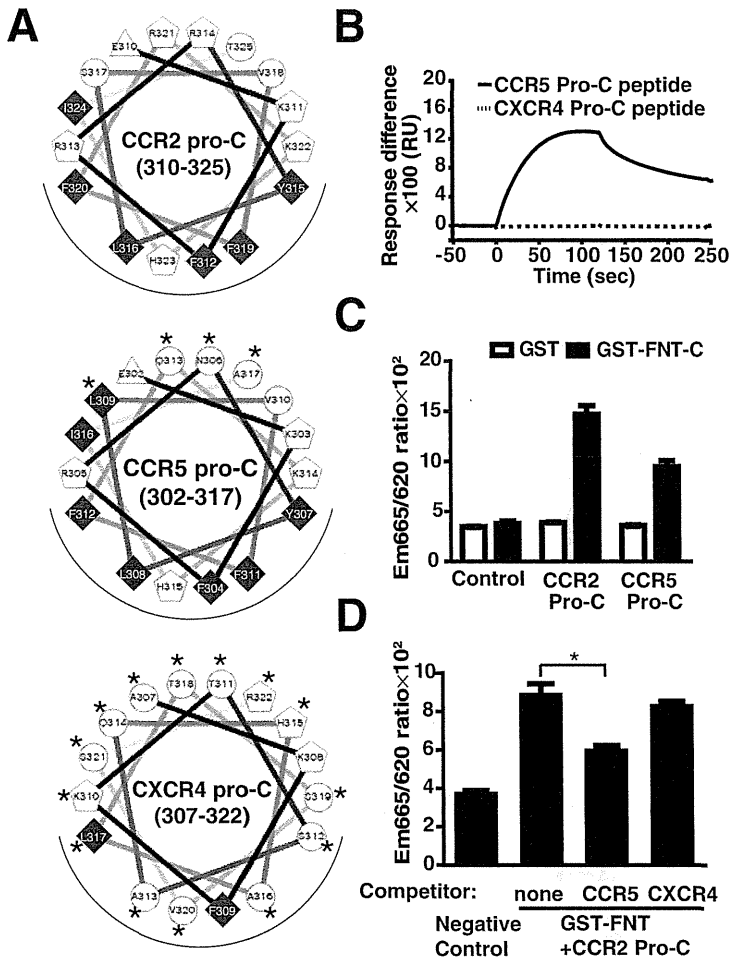

Figure 5 Common residues on the hydrophobic side of CCR2 Pro-C and CCR5 Pro-C and their role on FNT binding

(**A**) Helical wheel projections of the CCR2 pro-C region (amino acids 310–325) and the corresponding region of CCR5 and CXCR4. The hydrophobic residues are grey-coloured diamonds, hydrophilic residues are white circles, potentially negatively charged residues are white triangles and potentially positively charged residues are white pentagons. The asterisk indicates the amino acid distinct from that of CCR2. (**B**) The 16-amino acid peptides of CCR5, but not CXCR4, bound to the recombinant FNT-C protein in SPR analysis. (**C**) Interaction signals derived from the interaction between the biotinylated CCR2 Pro-C peptide or the biotinylated CCR5 Pro-C peptide and the recombinant FNT-C protein in a HTRF assay. (**D**) Competition assay using unlabelled CCR5 Pro-C or CXCR4 Pro-C at a concentration of 1 μM against the interaction of biotinylated CCR2 Pro-C peptide with FNT in a HTRF assay (means $\pm$ S.D.). $^*P < 0.05$.

helical state of the helix 8 region is responsible for binding to the cytoplasmic protein FNT (Figure 4); furthermore, residues on the hydrophobic side of the helix 8 region are completely conserved among the two FNT-binding receptors CCR2 and CCR5 (Figure 5). Previous reports have demonstrated important roles for the helix 8 region in receptor activation [26–28], although the molecular mechanisms remain unclear. The results of the present study provide new insight into the regulation mechanism mediated by helix 8, in which the hydrophobic side of helix 8 serves as a binding site for a cytoplasmic regulator. Based on our findings, together with previous findings, we propose a hypothesis that FNT, upon chemokine stimulation, accumulates to the plasma membrane to interact with the helix 8 region of chemokine receptors, promoting receptor clusterization and amplifying receptor signalling, leading to accurate formation of pseudopodia directed towards the chemokine concentration.

Chemokine receptors have been considered as potential drug targets because they have been reported to contribute to the onset and progression of cancer and inflammatory diseases [29]. The diversity among chemokines and chemokine receptors has been well documented over the past two decades since the discovery of chemokine prototypes [30–32]; by contrast, the diversity of cytoplasmic-binding molecules is not well understood. Besides its role in monocytes/macrophages, FNT is required for the migration and recruitment of CCR2-expressing bone marrow-derived mesenchymal stem cells to the injured heart [33]. FNT has also been reported to mediate the transendothelial migration of prostate carcinoma through activation of the small G-protein Rac [34]. Although the physiological dynamics of the receptor–FNT interaction should be further studied, our findings provide insight into the mechanism underlying the interaction of chemokine receptors with the cytoplasmic regulator FNT, and the interaction systems described in the present study would be useful tools for drug development targeting the interaction between CCR2/CCR5 and FNT.

In conclusion, our findings emphasize the importance of a short element at the membrane-proximal C-terminal region of chemokine receptors, and perhaps other GPCRs, for binding to

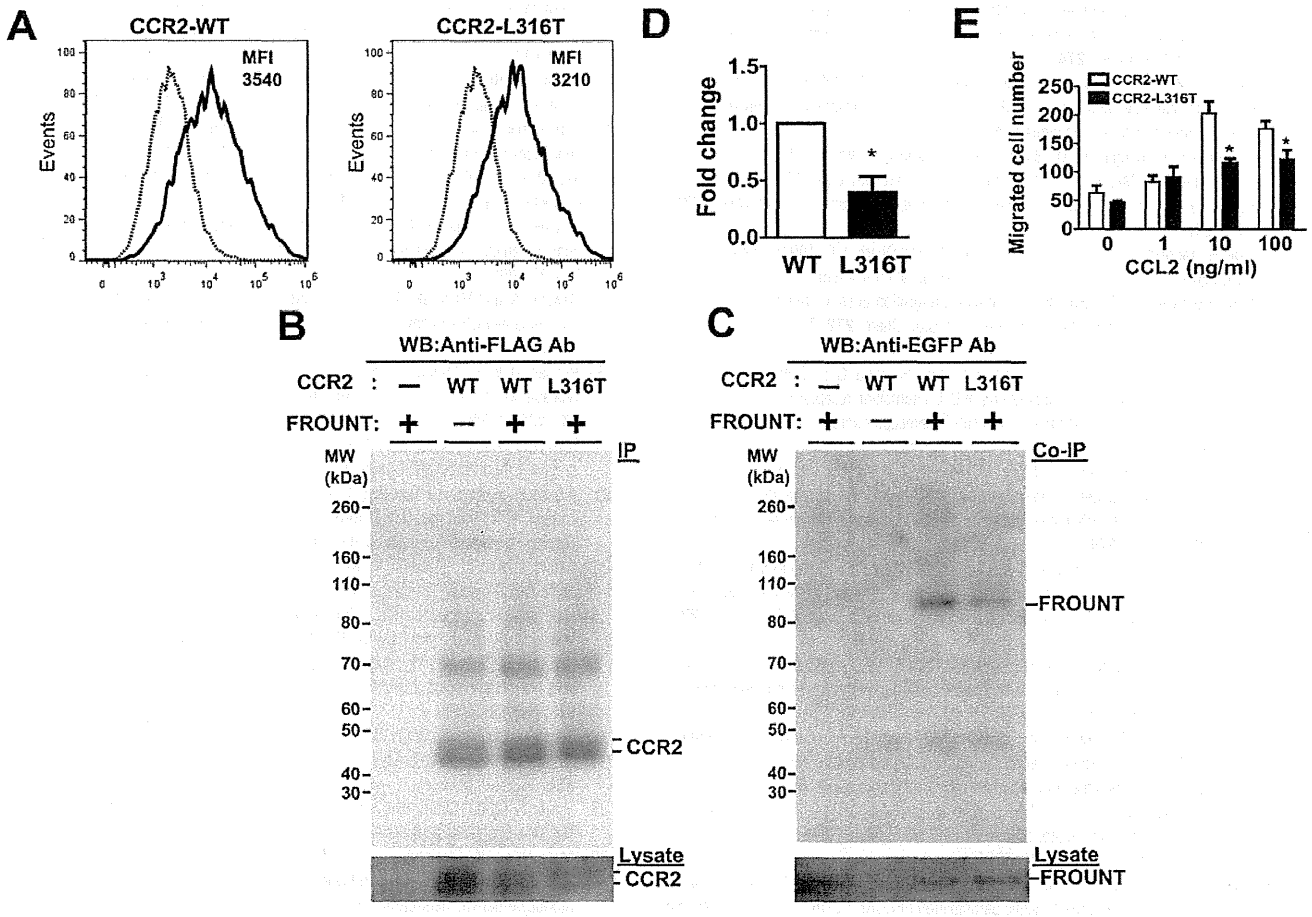

Figure 6 FNT-binding ability of full-length, wild-type or mutated CCR2 and chemotactic ability of cells expressing mutated CCR2

(**A**) Human CCR2 or CCR2-L316T tagged with FLAG and EGFP-tagged FNT were co-transfected into HEK-293 cells. GFP fluorescence derived from EGFP–FNT and surface expression of FLAG–CCR2 were measured by flow cytometry (solid line). The broken line indicates no transfected cells. Mean fluorescence intensities (MFI) are shown in each panel. (**B** and **C**) Immunoprecipitation (IP) of CCL2-stimulated transfected HEK-293 cell lysates was performed using an anti-FLAG antibody followed by a Western blot assay (WB). Immunoblots were probed with the anti-FLAG antibody to detect immunoprecipitation of wild-type CCR2 or CCR2-L316T (**B**), and with the anti-EGFP antibody to detect co-immunoprecipitation of EGFP–FNT (**C**). The immunoblot of each cell lysate is shown below. Molecular mass (MW) is given on the left-hand side in kDa. (**D**) Co-immunoprecipitation data from three independent experiments were quantified and normalized to the amount of each receptor immunoprecipitated and are shown as the fold change over the wild-type. (*$P < 0.05$). (**E**) Chemotaxis of Jurkat cells transfected with wild-type CCR2 (white bar) or CCR2-L316T (black bar). Cells that had migrated from the upper chamber to the lower chamber containing medium or CCL2 were counted under a fluorescence microscope. Results are means ± S.D. (*$P < 0.05$ compared with the wild-type CCR2).

cytoplasmic regulatory molecules. Identification of other proteins that bind to this region of other GPCRs may lead to further understanding of receptor activation mechanisms.

AUTHOR CONTRIBUTION

Etsuko Toda and Yuya Terashima conceived the study, performed the experiments, analysed the data and wrote the paper. Kaori Esaki, Sosuke Yoshinaga and Hiroaki Terasawa prepared the FNT protein and contributed to discussions. Yutaka Kofuku and Ichio Shimada assisted in the conduction of the SPR experiments using Biacore2000 and contributed with important advice to the paper. Minoru Sugihara and Makiko Suwa conducted the cluster analysis of GPCRs in the Supplementary Online Data and assisted in preparing the paper. Shiro Kanegasaki critically reviewed the paper prior to submission and Kouji Matsushima gave conceptual advice. Yuya Terashima directed the overall research. All authors read and approved the final paper.

ACKNOWLEDGEMENTS

We thank Kana Kokubo, Yuko Kobayashi, Ryu Takahashi, Taeko Ito, Mizuho Ishida, Masaru Ueda, Saeko Ohi, Yasushi Hiramatsu, Jutaro Kawaguchi, Yukimi Nakayama and Jumpei Shosaku for experimental help, and all the members of our laboratory for discussions and help.

FUNDING

This work was supported, in part, by the MEXT (Ministry of Education, Culture, Sports, Science and Technology) Japan via the TPRP (Targeted Proteins Research Programme) and the P-DIRECT (Project for Development of Innovative Research on Cancer Therapeutics) and a Grant-in-Aid for Young Scientists (B) [grant number 24790462 (to Y.T.)], and the JSPS (Japan Society for the Promotion of Science) [grant number 24-40099 (to E.T.)]

REFERENCES

1 Richardson, R. M., Ali, H., Pridgen, B. C., Haribabu, B. and Snyderman, R. (1998) Multiple signaling pathways of human interleukin-8 receptor A. Independent regulation by phosphorylation. J. Biol. Chem. **273**, 10690–10695

2 Ko, J., Jang, S. W., Kim, Y. S., Kim, I. S., Sung, H. J., Kim, H. H., Park, J. Y., Lee, Y. H., Kim, J. and Na, D. S. (2004) Human LZIP binds to CCR1 and differentially affects the chemotactic activities of CCR1-dependent chemokines. FASEB J. **18**, 890–892

3 Sambrano, G. R. and Coughlin, S. R. (1999) The carboxyl tail of protease-activated receptor-1 is required for chemotaxis. Correlation of signal termination and directional migration. J. Biol. Chem. **274**, 20178–20184
4 Fan, G. H., Yang, W., Wang, X. J., Qian, Q. and Richmond, A. (2001) Identification of a motif in the carboxyl terminus of CXCR2 that is involved in adaptin 2 binding and receptor internalization. Biochemistry **40**, 791–800
5 Ben-Baruch, A., Bengali, K. M., Biragyn, A., Johnston, J. J., Wang, J. M., Kim, J., Chuntharapai, A., Michiel, D. F., Oppenheim, J. J. and Kelvin, D. J. (1995) Interleukin-8 receptor β. The role of the carboxyl terminus in signal transduction. J. Biol. Chem. **270**, 9121–9128
6 Arai, H., Monteclaro, F. S., Tsou, C. L., Franci, C. and Charo, I. F. (1997) Dissociation of chemotaxis from agonist-induced receptor internalization in a lymphocyte cell line transfected with CCR2B. Evidence that directed migration does not require rapid modulation of signaling at the receptor level. J. Biol. Chem. **272**, 25037–25042
7 Gosling, J., Monteclaro, F. S., Atchison, R. E., Arai, H., Tsou, C. L., Goldsmith, M. A. and Charo, I. F. (1997) Molecular uncoupling of C-C chemokine receptor 5-induced chemotaxis and signal transduction from HIV-1 coreceptor activity. Proc. Natl. Acad. Sci. U.S.A. **94**, 5061–5066
8 Kraft, K., Olbrich, H., Majoul, I., Mack, M., Proudfoot, A. and Oppermann, M. (2001) Characterization of sequence determinants within the carboxyl-terminal domain of chemokine receptor CCR5 that regulate signaling and receptor internalization. J. Biol. Chem. **276**, 34408–34418
9 Venkatesan, S., Petrovic, A., Locati, M., Kim, Y. O., Weissman, D. and Murphy, P. M. (2001) A membrane-proximal basic domain and cysteine cluster in the C-terminal tail of CCR5 constitute a bipartite motif critical for cell surface expression. J. Biol. Chem. **276**, 40133–40145
10 Sai, J., Fan, G. H., Wang, D. and Richmond, A. (2004) The C-terminal domain LLKIL motif of CXCR2 is required for ligand-mediated polarization of early signals during chemotaxis. J. Cell Sci. **117**, 5489–5496
11 Terashima, Y., Onai, N., Murai, M., Enomoto, M., Poonpiriya, V., Hamada, T., Motomura, K., Suwa, M., Ezaki, T., Haga, T. et al. (2005) Pivotal function for cytoplasmic protein FROUNT in CCR2-mediated monocyte chemotaxis. Nat. Immunol. **6**, 827–835
12 Toda, E., Terashima, Y., Sato, T., Hirose, K., Kanegasaki, S. and Matsushima, K. (2009) FROUNT is a common regulator of CCR2 and CCR5 signaling to control directional migration. J. Immunol. **183**, 6387–6394
13 Murai, M., Yoneyama, H., Harada, A., Yi, Z., Vestergaard, C., Guo, B., Suzuki, K., Asakura, H. and Matsushima, K. (1999) Active participation of $CCR5^+$ $CD8^+$ T lymphocytes in the pathogenesis of liver injury in graft-versus-host disease. J. Clin. Invest. **104**, 49–57
14 Boring, L., Gosling, J., Cleary, M. and Charo, I. F. (1998) Decreased lesion formation in $CCR2^{-/-}$ mice reveals a role for chemokines in the initiation of atherosclerosis. Nature **394**, 894–897
15 Fife, B. T., Huffnagle, G. B., Kuziel, W. A. and Karpus, W. J. (2000) CC chemokine receptor 2 is critical for induction of experimental autoimmune encephalomyelitis. J. Exp. Med. **192**, 899–905
16 Izikson, L., Klein, R. S., Charo, I. F., Weiner, H. L. and Luster, A. D. (2000) Resistance to experimental autoimmune encephalomyelitis in mice lacking the CC chemokine receptor (CCR)2. J. Exp. Med. **192**, 1075–1080
17 Esaki, K., Terashima, Y., Toda, E., Yoshinaga, S., Araki, N., Matsushima, K. and Terasawa, H. (2011) Expression and purification of human FROUNT, a common cytosolic regulator of CCR2 and CCR5. Protein Expr. Purif. **77**, 86–91
17a Suwa, M. and Ono, Y. (2009) Computational overview of GPCR gene universe to support reverse chemical genomics study. Methods Mol. Biol. **577**, 41–54
18 Sugihara, M., Fujibuchi, W. and Suwa, M. (2011) Structural elements of the signal propagation pathway in squid rhodopsin and bovine rhodopsin. J. Phys. Chem. B **115**, 6172–6179
19 Pontius, J., Richelle, J. and Wodak, S. J. (1996) Deviations from standard atomic volumes as a quality measure for protein crystal structures. J. Mol. Biol. **264**, 121–136
20 Zimmerman, J. M., Eliezer, N. and Simha, R. (1968) The characterization of amino acid sequences in proteins by statistical methods. J. Theor. Biol. **21**, 170–201
21 Kyte, J. and Doolittle, R. F. (1982) A simple method for displaying the hydropathic character of a protein. J. Mol. Biol. **157**, 105–132
22 Fauchère, J. L., Charton, M., Kier, L. B., Verloop, A. and Pliska, V. (1988) Amino acid side chain parameters for correlation studies in biology and pharmacology. Int. J. Pept. Protein Res. **32**, 269–278
23 Sawano, A. and Miyawaki, A. (2000) Directed evolution of green fluorescent protein by a new versatile PCR strategy for site-directed and semi-random mutagenesis. Nucleic Acids Res. **28**, E78
23a Buchan, D. W. A., Minneci, F., Nugent, T. C. O., Bryson, K. and Jones, D. T. (2013) Scalable web services for the PSIPRED protein analysis workbench. Nucleic Acids Res. **41**, W340–W348
24 Raman, D., Sai, J., Neel, N. F., Chew, C. S. and Richmond, A. (2010) LIM and SH3 protein-1 modulates CXCR2-mediated cell migration. PLoS ONE **5**, e10050
25 Alonzo, F., Kozhaya, L., Rawlings, S. A., Reyes-Robles, T., DuMont, A. L., Myszka, D. G., Landau, N. R., Unutmaz, D. and Torres, V. J. (2013) CCR5 is a receptor for *Staphylococcus aureus* leukotoxin ED. Nature **493**, 51–55
26 Okuno, T., Ago, H., Terawaki, K., Miyano, M., Shimizu, T. and Yokomizo, T. (2003) Helix 8 of the leukotriene B4 receptor is required for the conformational change to the low affinity state after G-protein activation. J. Biol. Chem. **278**, 41500–41509
27 Verzijl, D., Pardo, L., van Dijk, M., Gruijthuijsen, Y. K., Jongejan, A., Timmerman, H., Nicholas, J., Schwarz, M., Murphy, P. M., Leurs, R. and Smit, M. J. (2006) Helix 8 of the viral chemokine receptor ORF74 directs chemokine binding. J. Biol. Chem. **281**, 35327–35335
28 Feierler, J., Wirth, M., Welte, B., Schüssler, S., Jochum, M. and Faussner, A. (2011) Helix 8 plays a crucial role in bradykinin B_2 receptor trafficking and signaling. J. Biol. Chem. **286**, 43282–43293
29 Horuk, R. (2009) Chemokine receptor antagonists: overcoming developmental hurdles. Nat. Rev. Drug Discov. **8**, 23–33
30 Matsushima, K., Morishita, K., Yoshimura, T., Lavu, S., Kobayashi, Y., Lew, W., Appella, E., Kung, H. F., Leonard, E. J. and Oppenheim, J. J. (1988) Molecular cloning of a human monocyte-derived neutrophil chemotactic factor (MDNCF) and the induction of MDNCF mRNA by interleukin 1 and tumor necrosis factor. J. Exp. Med. **167**, 1883–1893
31 Yoshimura, T., Yuhki, N., Moore, S. K., Appella, E., Lerman, M. I. and Leonard, E. J. (1989) Human monocyte chemoattractant protein-1 (MCP-1). Full-length cDNA cloning, expression in mitogen-stimulated blood mononuclear leukocytes, and sequence similarity to mouse competence gene JE. FEBS Lett. **244**, 487–493
32 Furutani, Y., Nomura, H., Notake, M., Oyamada, Y., Fukui, T., Yamada, M., Larsen, C. G., Oppenheim, J. J. and Matsushima, K. (1989) Cloning and sequencing of the cDNA for human monocyte chemotactic and activating factor (MCAF). Biochem. Biophys. Res. Commun. **159**, 249–255
33 Belema-Bedada, F., Uchida, S., Martire, A., Kostin, S. and Braun, T. (2008) Efficient homing of multipotent adult mesenchymal stem cells depends on FROUNT-mediated clustering of CCR2. Cell Stem Cell. **2**, 566–575
34 van Golen, K. L., Ying, C., Sequeira, L., Dubyk, C. W., Reisenberger, T., Chinnaiyan, A. M., Pienta, K. J. and Loberg, R. D. (2008) CCL2 induces prostate cancer transendothelial cell migration via activation of the small GTPase Rac. J. Cell Biochem. **104**, 1587–1597

Received 26 June 2013/8 October 2013; accepted 15 October 2013
Published as BJ Immediate Publication 15 October 2013, doi:10.1042/BJ20130827

IJC
International Journal of Cancer

Adoptive cytotoxic T lymphocyte therapy triggers a counter-regulatory immunosuppressive mechanism *via* recruitment of myeloid-derived suppressor cells

Akihiro Hosoi[1,2], Hirokazu Matsushita[1], Kanako Shimizu[3], Shin-ichiro Fujii[3], Satoshi Ueha[4], Jun Abe[4], Makoto Kurachi[4], Ryuji Maekawa[2], Kouji Matsushima[4] and Kazuhiro Kakimi[1]

[1] Department of Immunotherapeutics, The University of Tokyo Hospital, Tokyo, Japan
[2] MEDINET Co., Ltd. Yokohama, Japan
[3] Research Unit for Cellular Immunotherapy, The Institute of Physical and Chemical Research (RIKEN), Research Center for Allergy and Immunology (RCAI), Yokohama, Japan
[4] Department of Molecular Preventive Medicine, Graduate School of Medicine, The University of Tokyo, Tokyo, Japan

Complex interactions among multiple cell types contribute to the immunosuppressive milieu of the tumor microenvironment. Using a murine model of adoptive T-cell immunotherapy (ACT) for B16 melanoma, we investigated the impact of tumor infiltrating cells on this complex regulatory network in the tumor. Transgenic pmel-1-specific cytotoxic T lymphocytes (CTLs) were injected intravenously into tumor-bearing mice and could be detected in the tumor as early as on day 1, peaking on day 3. They produced IFN-γ, exerted anti-tumor activity and inhibited tumor growth. However, CTL infiltration into the tumor was accompanied by the accumulation of large numbers of cells, the majority of which were $CD11b^+Gr1^+$ myeloid-derived suppressor cells (MDSCs). Notably, $CD11b^+Gr1^{int}Ly6G^-Ly6C^+$ monocytic MDSCs outnumbered the CTLs by day 5. They produced nitric oxide, arginase I and reactive oxygen species, and inhibited the proliferation of antigen-specific $CD8^+$ T cells. The anti-tumor activity of the adoptively-transferred CTLs and the accumulation of MDSCs both depended on IFN-γ production on recognition of tumor antigens by the former. In $CCR2^{-/-}$ mice, monocytic MDSCs did not accumulate in the tumor, and inhibition of tumor growth by ACT was improved. Thus, ACT triggered counter-regulatory immunosuppressive mechanism *via* recruitment of MDSCs. Our results suggest that strategies to regulate the treatment-induced recruitment of these MDSCs would improve the efficacy of immunotherapy.

Tumor Immunology

Adoptive T-cell immunotherapy (ACT) is recognized as a potent therapy for cancer.[1,2] Using gene transfer technologies, host T cells can be modified to stably express exogenous T-cell receptors (TCRs)[3,4] or chimeric antigen receptors (CARs)[5–7] that redirects their reactivity toward tumor-associated antigens. Many phase I and II clinical trials using tumor-infiltrating lymphocytes have now been conducted, as well some with such genetically engineered T cells.[1,8] However, several crucial hurdles need to be overcome for the successful application of ACT. Tumors employ numerous different strategies to evade immune responses, including impaired antigen presentation, expression of ligands for negative costimulatory receptors on T cells (*e.g.* PD-L1, B7-H4), secretion of immunosuppressive factors (eg. IL-10, TGF-β, galectin-1, gangliosides, PGE2), ligands and factors for pro-apoptotic pathways (eg. FasL, TRAIL, IDO) and induction of regulatory cell populations, such as $CD4^+CD25^+$ regulatory T cells (Tregs), inducible Tr1 cells, IL-13-producing natural killer T (NKT) cells, and myeloid-derived suppressor cells (MDSC).[9,10] All these local events contribute to the establishment of a suppressive milieu in the tumor microenvironment which affects the anti-tumor activity of infiltrating immune cells. This results in a state of functional tolerance, defined as the coexistence of tumor-specific T cells and growing tumor cells.

To elicit efficient anti-tumor activities of transferred cytotoxic T lymphocytes (CTLs) and/or augmentation of their functions, further clarification of these tumor evasion strategies during ACT is required. Here, we investigated the intratumoral cellular immune response induced by the tumor-infiltrating adoptively-transferred CTLs using the B16-pmel-1 model.[11,12] We found that the anti-tumor activity of the infiltrating

Key words: CTL, MDSC, immunotherapy, adoptive transfer

Abbreviations: ACT: adoptive T cell immunotherapy; CTL: cytotoxic T lymphocyte; MDSC: myeloid-derived suppressor cell; DC: dendritic cell; Tregs: regulatory T cells; NKT: natural killer T; GM-CSF: granulocyte-macrophage colony stimulating factor

Additional Supporting Information may be found in the online version of this article.

Grant sponsor: Grant-in-Aid for Scientific Research of the Ministry of Education, Culture, Sports, Science and Technology (to K.K.)
DOI: 10.1002/ijc.28506
History: Received 18 May 2013; Accepted 12 Sep 2013; Online 6 Oct 2013

Correspondence to: Kazuhiro Kakimi, Department of Immunotherapeutics, The University of Tokyo Hospital, 7-3-1 Hongo, Bunkyo-Ku, Tokyo 113-8655, Japan, Tel.: 81-35805-3161, Fax: 81-35805-3164, E-mail: kakimi@m.u-tokyo.ac.jp

What's new?
One approach to immunotherapy is to engineer a patient/s own cytotoxic lymphocytes (CTLs) to express receptors for tumor-associated antigens. However, tumors often develop strategies to evade the anti-tumor activity of these immune cells. In this study using a mouse model of melanoma, the authors found that the efficacy of transgenic CTLs was blocked due to a massive accumulation of myeloid-derived suppressor cells (MDSCs) in the tumor. Surprisingly, this suppression was caused by IFN-γ produced by the CTLs themselves. These results suggest that strategies to regulate this treatment-induced recruitment of MDSCs could improve the efficacy of immunotherapy.

CTLs was compromised by massive accumulation of $CD11b^+Gr1^{int}Ly6C^+$ monocytic MDSCs in the tumor under the influence of the IFN-γ produced by the CTLs themselves.

Material and Methods

Mice, tumor cells and peptides

Male C57BL/6 mice at the age of 6 to 8 weeks were obtained from Japan SLC (Sizuoka, Japan) and used for dendritic cell (DC) preparation or as tumor-bearing mice in the ACT experiments. Mice transgenic for the Pmel-1-TCR recognizing the H-$2D^b$-restricted epitope EGSRNQDWL from gp100 (gp100 25-33) were obtained from The Jackson Laboratory (Bar Harbor, ME).[11] These mice are homozygous for the T lymphocyte-specific Thy1a (Thy1.1) allele. $CCR2^{-/-}$ mice were also purchased from The Jackson Laboratory and back-crossed for more than 10 generations onto the C57BL/6 background. All mice were housed in a pathogen-free environment.[13] All animal procedures were conducted in accordance with institutional guidelines. B16F10 is a gp100-positive spontaneous murine melanoma cell line, kindly provided by Dr. N. Restifo (National Cancer Institute) and maintained in culture medium consisting of DMEM (Wako Pure Chemical, Osaka, Japan) with 10% heat-inactivated fetal bovine serum (Bio West, Nuaillé, France), 100 μg/ml streptomycin and 100 U/ml penicillin (Wako Pure Chemical). The H-$2D^b$–restricted peptide human gp100 (hgp100 25–33, KVPRNQDWL) was purchased from GenScript Japan (Tokyo, Japan) at a purity of >90%, with a free amino terminal and carboxyl terminal.

DC preparation and CTL stimulation

DCs were obtained by 8-day culture of C57BL/6-derived bone marrow cells with granulocyte-macrophage colony stimulating factor (GM-CSF) as described previously.[14] Briefly, bone marrow cells obtained from tibias and femurs of C57BL/6 mice were cultured in RPMI 1640 medium supplemented with 10% FCS, 12.5 mM HEPES, 5×10^{-5} M 2-mercaptoethanol, 1×10^{-5} M sodium pyruvate, 1% nonessential amino acids, 100 U/ml penicillin, 100 μg/ml streptomycin and 20 ng/ml GM-CSF (PeproTech, Rocky Hill, NJ) for 8 days. On days 3 and 6, half the medium was replaced with fresh medium containing GM-CSF. DCs were further incubated with lipopolysaccharide (1 μg/ml) for 16 hr and then pulsed with hgp100 peptide (1 μg/ml) for 3 hr to obtain peptide-pulsed mature DCs. Spleen cells (1×10^7) from pmel-1-TCR transgenic mice were co-cultured with these DCs (2×10^5) for 3 days in medium containing 50 U/ml IL-2 (Chiron Corporation, Emeryville, CA) to prepare CTLs. After 3 days *in vitro* stimulation, approximately 90% of the harvested cells were $CD3^+CD8^+$ CTLs. Therefore, no further purification was performed before ACT.

ACT and anti-IFN-γ mAb treatment

C57BL/6 mice or $CCR2^{-/-}$ mice were first inoculated with 1×10^6 B16F10 cells subcutaneously on day 0, followed by adoptive CTL transfer (1×10^7) on day 9. Tumor growth was monitored every 2 to 3 days with calipers in a blinded fashion and was performed independently at least twice with similar results. On the day of, and 2 days after, CTL transfer, mice received intraperitoneal injections of 500 μg anti-IFN-γ mAb (clone XMG1.2, BioXCell, West Lebanon, NH) or rat IgG_1 isotype control (BioXCell). Tumor volume was calculated by the formula $\pi/6 \times L_1L_2H$, where L_1 is the long diameter, L_2 is the short diameter, and H is the height of the tumor. Survival was monitored periodically. Tumor-bearing mice either died or had to be euthanized when the tumor volume exceeded approximately 1,500 mm^3.

Cell preparation and flow cytometry

Tumors were harvested from mice at different time points, cut into pieces, and re-suspended in HBSS supplemented with 0.1% collagenase D (Roche Diagnostics, Indianapolis, IN) and DNase I (Roche Diagnostics) for 60 min at 37°C. The entire material was passed through a 70 μm cell strainer (BD Falcon, BD Bioscience) by being pressed with a plunger, to obtain single cell suspensions of tumor-infiltrating cells. For flow cytometry, these tumor digests were used without density gradient purification. The cells were first stained with Fixable Viability Dye eFluor450 (eBioscience, San Diego, CA) to label dead cells, and were pretreated with Fc Block (anti-CD16/32 clone 2.4G2; BD Pharmingen). The cells were then stained with antibodies and analyzed on a Gallios™ flow cytometer (Beckman Coulter, San Diego, CA). The following mAbs were obtained from BioLegend (San Diego, CA) and used for flow cytometry: FITC- or PerCP/Cy5.5-conjugated anti-CD45, PE-conjugated anti-NK1.1, Ly6G, PE/Cy7–conjugated anti-Ly6C, Alexa Fluor647-conjugated anti-CD90.1, APC-conjugated anti-CD107a, biotin-conjugated anti-Gr1, IL4Rα, F4/80, and Streptavidin-APC, APC-Cy7-conjugated anti-CD8, CD11b, Pacific Blue-conjugated anti-CD45. Data